Causal structure of bigravity solutions

D. Blas[c1], C. Deffayet[a,b,2], J. Garriga[c,3],

[a]APC [4], 11 place Marcelin Berthelot,

75005 Paris Cedex 05, France.

[b] GReCO/IAP [5] 98 bis boulevard Arago, 75014 Paris, France.

[c]Departament de Física Fonamental, Universitat de Barcelona,

Diagonal 647, 08028 Barcelona, Spain.

Abstract

We discuss the causal diagrams of static and spherically symmetric bigravity vacuum solutions, with interacting metrics f and g. Such solutions can be classified into type I (or "non-diagonal") and type II (or "diagonal"). The general solution of type I is known, and leads to metrics f and g in the Schwarzschild-(Anti)de Sitter family. The two metrics are not always diagonalizable in the same coordinate system, and the light-cone structure of both metrics can be quite different. In spite of this, we find that causality is preserved, in the sense that closed time-like curves cannot be pieced together from geodesics of both metrics. We propose maximal extensions of Type I bigravity solutions, where geodesics of both metrics do not stop unless a curvature singularity is encountered. Such maximal extensions can contain several copies (or even an infinite number of them) of the maximally extended "individual" geometries associated to f and g separately. Generically, we find that the maximal extensions of bigravity solutions are not globally hyperbolic, even in cases when the individual geometries are. The general solution of type II has not been given in closed form. We discuss a subclass where g is an arbitrary solution of Einstein's equations with a cosmological constant, and we find that in this case the only solutions are such that $f \propto g$ (with trivial causal structure).

[1]dblas@ffn.ub.es

[2]deffayet@iap.fr

[3]garriga@ifae.es

[4]UMR 7164 (CNRS, Université Paris 7, CEA, Observatoire de Paris)

[5]UMR 7095 (CNRS, Université Paris 6)

1 Introduction

Recently, massive gravity, and other infrared modifications of General Relativity, have been the subject of numerous investigations[1, 2, 3, 4, 5], largely motivated by the enigma of dark energy[6, 7, 8]. A linearized ghost-free theory of massive gravity can be constructed by adding a suitable quadratic mass term to the linearized Einstein Lagrangian. This is the so-called Pauli-Fierz theory (PF) [9]. Non-linear and generally covariant extensions can easily be formulated, at the cost of introducing new fields. The simplest possibility is to consider the theory of two metrics, f and g, with standard kinetic terms, where the mass terms arise from non-derivative interactions between f and g. This is known as bigravity, $f - g$ theory, or *strong gravity*, and was first considered in the seventies, in the context of the strong interactions [10][6]. Massive gravity poses certain difficulties. First of all, the linearized theory does not agree with observations. The PF Lagrangian propagates a scalar degree of freedom (in addition to two tensor and two vector polarizations) which couples to matter with gravitational strength. The coupling persists in the limit as the graviton mass vanishes, causing the so-called vDVZ discontinuity [13]. It has been suggested that the discontinuity may disappear due to non-linear effects [14], in the sense that solutions of massless gravity can be recovered non-perturbatively. This mechanism may indeed work in more complicated infrared modifications of gravity, such as the theories discussed in [15], although its implementation in the context of bigravity may be problematic (see e.g. [16]). In addition, the minimal non linear extension of PF theory was found to propagate six degrees of freedom rather than five [17], the sixth degree of freedom being ghost like. This increase in the number of propagating degrees of freedom was also found to occur in bigravity [2], and in general, it may be related to the strong self-interaction of the scalar polarization of the graviton [18, 19].

Despite such difficulties, bigravity remains an elegant framework where to investigate the massive graviton, particularly because a large class of exact solutions to this theory are known. Interestingly, there are solutions where both metrics f and g belong to the Schwarzschild-(Anti) de Siter family, which makes them phenomenologically attractive. On the other hand, in dealing with a space-time with two metrics, it is natural to ask whether we can make sense of its causal structure. In general, the light-cones generated by metrics f and g will not agree, and this may lead to pathologies which may restrict the class of physically acceptable solutions. The purpose of this paper is to investigate this issue in some detail.

In Section 2, we review the classification of static spherically symmetric solutions of bigravity. These fall into two types. In type I solutions, the area of orbits of spherical symmetry as measured by the f metric is $2/3$ of the area as measured by the g metric. Otherwise, the solutions are called type II. In type II solutions, both metrics can be brought to diagonal form in the same coordinate system, whereas this is not always possible in type I solutions, where only one of them can be diagonalized at a time. The general solution of type I was given in early work [20, 21, 16]. The general solution of type II is not known explicitly [22]. We shall consider the subclass where one of the metrics is a solution of Einstein's equations with a cosmological constant, for which we discuss the general solution. In Section 3, we discuss the causal structure of type I solutions. Section 4 summarizes our conclusions. Some technical issues concerning type II solutions are left to an Appendix.

---

[6]Bigravity (and multigravity in general) is also relevant to the program of "deconstruction" of gravity [11, 12]

2 Spherically symmetric solutions in bigravity

As mentioned in the introduction all type I solutions are known analytically, while the general type II solution is not known. In this Section, we review this classification, and comment on a subset of type II solutions.

Following [10], we consider the action

$$S = \int \mathrm{d}^4x \sqrt{-g} \left(\frac{-R_g}{2\kappa_g} + L_g \right) + \int \mathrm{d}^4x \sqrt{-f} \left(\frac{-R_f}{2\kappa_f} + L_f \right) + S_{int}[f,g] \tag{1}$$

Here L_f and L_g denote generic matter Lagrangians coupled to the metrics f and g respectively. In solving the field equations, we shall restrict attention to the case where there is only a vacuum energy term in each matter sector $L_f = -\rho_f, L_g = -\rho_g$. There is much freedom in the choice of the interaction term in (1). For definiteness, we shall consider the form [10]

$$S_{int} = -\frac{\zeta}{4} \int \mathrm{d}^4x (-g)^u (-f)^v (f^{\mu\nu} - g^{\mu\nu})(f^{\sigma\tau} - g^{\sigma\tau})(g_{\mu\sigma}g_{\mu\tau} - g_{\mu\nu}g_{\sigma\tau}) \tag{2}$$

with

$$u + v = \frac{1}{2}. \tag{3}$$

This reduces to the Pauli-Fierz one in the linear regime, when g is taken to be the Minkowski metric (but many other choices could be made with this same property [2]). The equations of motion, derived from action (1), read

$$G^f_{\mu\nu} = \kappa_f T^f_{\mu\nu}, \qquad G^g_{\mu\nu} = \kappa_g T^g_{\mu\nu}, \tag{4}$$

where $G_{\mu\nu}$ denotes the Einstein tensor, and the energy-momentum tensors are given by

$$T^f_{\mu\nu} = \frac{\zeta}{2} \left(\frac{g}{f} \right)^u \left[v f_{\mu\nu}(f^{\alpha\beta} - g^{\alpha\beta})(f^{\sigma\tau} - g^{\sigma\tau})(g_{\alpha\sigma}g_{\beta\tau} - g_{\alpha\beta}g_{\sigma\tau}) \right.$$
$$\left. -2(f^{\alpha\beta} - g^{\alpha\beta})(g_{\mu\alpha}g_{\beta\nu} - g_{\mu\nu}g_{\alpha\beta}) \right] + \rho_f f_{\mu\nu} \tag{5}$$

$$T^g_{\mu\nu} = \frac{\zeta}{2} \left(\frac{f}{g} \right)^v \left[(f^{\alpha\beta} - g^{\alpha\beta})(f^{\sigma\tau} - g^{\sigma\tau})(u g_{\mu\nu}g_{\alpha\sigma}g_{\beta\tau} - u g_{\mu\nu}g_{\alpha\beta}g_{\sigma\tau} + 2 g_{\mu\alpha}g_{\sigma\nu}g_{\beta\tau} - 2 g_{\mu\alpha}g_{\nu\beta}g_{\sigma\tau}) \right.$$
$$\left. +2(f^{\alpha\beta} - g^{\alpha\beta})(g_{\mu\alpha}g_{\beta\nu} - g_{\mu\nu}g_{\alpha\beta}) \right] + \rho_g g_{\mu\nu} \tag{6}$$

Let us now concentrate on static spherically symmetric solutions. By suitable choice of coordinates, the most general static and spherically symmetric ansatz for bigravity can be cast into the form

$$g_{\mu\nu}\mathrm{d}x^\mu \mathrm{d}x^\nu = J\mathrm{d}t^2 - K\mathrm{d}r^2 - r^2 \left(\mathrm{d}\theta^2 + \sin^2\theta \,\mathrm{d}\phi^2 \right) \tag{7}$$
$$f_{\mu\nu}\mathrm{d}x^\mu \mathrm{d}x^\nu = C\mathrm{d}t^2 - 2D\mathrm{d}t\mathrm{d}r - A\mathrm{d}r^2 - B \left(\mathrm{d}\theta^2 + \sin^2\theta \,\mathrm{d}\phi^2 \right), \tag{8}$$

where the metric coefficients are functions of r. As noted in Ref. [21], with the present ansatz we have

$$DG^f_{tt} + CG^f_{tr} = 0. \tag{9}$$

3

Hence, from the equations of motion, the following combination of components of the energy momentum tensor T^f must also vanish

$$DT_{tt}^f + CT_{tr}^f = -\frac{\zeta DJ}{2B}\left(\frac{JKr^4}{\Delta B^2}\right)^u (3B - 2r^2) = 0. \tag{10}$$

Here, we have introduced $\Delta = AC + D^2$ [21]. There are two different ways of satisfying this equality. Either

$$B = \frac{2}{3}r^2, \tag{11}$$

or

$$D = 0. \tag{12}$$

Solutions obeying the first condition (11) are called type I, and they were first discussed in [20]. The remaining ones are called type II and, from (12), they are necessarily diagonal. Let us discuss both types of solutions in turn.

2.1 Type I solutions

In the case when the vacuum energies of matter fields vanish, the general solution of type I was given in [20, 21]. The same method can be used in the case when ρ_f and ρ_g are nonvanishing, and one readily finds that the general solution is of the form

$$g_{\mu\nu}\mathrm{d}x^\mu\mathrm{d}x^\nu = (1 - q)\,\mathrm{d}t^2 - (1 - q)^{-1}\mathrm{d}r^2 - r^2(\mathrm{d}\theta^2 + \sin^2\theta\mathrm{d}\phi^2) \tag{13}$$

$$f_{\mu\nu}\mathrm{d}x^\mu\mathrm{d}x^\nu = \frac{2}{3\beta}(1 - p)\mathrm{d}t^2 - 2D\mathrm{d}t\mathrm{d}r - A\mathrm{d}r^2 - \frac{2}{3}r^2(\mathrm{d}\theta^2 + \sin^2\theta\mathrm{d}\phi^2), \tag{14}$$

where

$$A = \frac{2}{3\beta}(1 - q)^{-2}\left(p + \beta - q - \beta q\right), \tag{15}$$

$$D^2 = \left(\frac{2}{3\beta}\right)^2(1 - q)^{-2}(p - q)(p + \beta - 1 - \beta q). \tag{16}$$

Here $\beta > 0$ is an arbitrary constant, and the potentials p and q are functions of r. Substituting this ansatz into the expresions (5-6), it can be checked that the energy momentum tensors take the form of cosmological terms: $T_{\mu\nu}^f = (\Lambda_f/\kappa_f)f_{\mu\nu}$, and $T_{\mu\nu}^g = (\Lambda_g/\kappa_g)g_{\mu\nu}$, where

$$\frac{\Lambda_f}{\kappa_f} = \frac{\zeta}{4}\left(\frac{3}{2}\right)^{4u}\beta^u\left\{3v + 9\beta(1 - v)\right\} + \rho_f, \tag{17}$$

$$\frac{\Lambda_g}{\kappa_g} = \frac{\zeta}{4}\left(\frac{2}{3}\right)^{4v}\beta^{-v}\left\{3u - 9\beta(1 + u)\right\} + \rho_g. \tag{18}$$

It is clear from the equations of motion (4) that the metrics f and g must belong to the Schwarzschild-(A)dS family. Note that the corresponding cosmological constants (17-18) are not determined

4

solely by the vacuum energies ρ_f and ρ_g. They also contain a contribution from the interaction term in the Lagrangian. This contribution depends not only on the parameters ζ and u (recall that $v = 1/2 - u$), but also on the arbitrary integration constant β.

It is somewhat surprising that the cosmological constants depend on an integration constant. This situation is reminiscent of unimodular gravity, where the equations of motion are the traceless part of Einstein's equations. In this case, the vacuum energy does not determine the trace of the Ricci scalar [23] and Einstein's equations are recovered after using of the Bianchi identities except for an arbitrary integration constant that can chosen at will [24] (see also [25]). One difference here is that we have two cosmological constants Λ_f and Λ_g, and we can only choose the value of one of them at will.

The metric (14) can be put in a more familiar form defining a new time coordinate $\tilde{t}$ by

$$\mathrm{d}\tilde{t} = \frac{1}{\sqrt{\beta}} \left\{ \mathrm{d}t + \epsilon_D \frac{\sqrt{(p-q)(p+\beta-1-\beta q)}}{(1-q)(1-p)} \mathrm{d}r \right\}, \tag{19}$$

where $\epsilon_D = \pm 1$ is defined by the sign retained for D from equation (14), namely by

$$D = -\epsilon_D \frac{2}{3\beta}(1-q)^{-1}\sqrt{(p-q)(p+\beta-1-\beta q)}. \tag{20}$$

With such a coordinate change, the line element (14) now reads

$$f_{\mu\nu}\mathrm{d}x^\mu \mathrm{d}x^\nu = \frac{2}{3}\{(1-p)\mathrm{d}\tilde{t}^2 - (1-p)^{-1}\mathrm{d}r^2 - r^2(\mathrm{d}\theta^2 + \sin^2\theta \mathrm{d}\phi^2)\}. \tag{21}$$

As is clear from the previous discussion, the potentials p and q will be given by the familiar Schwarzschild-(A)dS forms

$$p = \frac{2M_f}{r} + \frac{2\Lambda_f}{9}r^2, \tag{22}$$

$$q = \frac{2M_g}{r} + \frac{\Lambda_g}{3}r^2, \tag{23}$$

where M_f and M_g are two additional integration constants with the interpretation of mass parameters.

It is tempting to conclude that this non-linear "theory of massive gravity" is phenomenologically sound, since the vacuum solutions of General Relativity with a cosmological term are recovered, without a trace of the vDVZ discontinuity. In this sense, the mass term does not seem to act as an exponential cut-off at a finite range. Rather, it contributes to the effective cosmological constant, which tends to bend space-time on a lengthscale of the order of the inverse mass of the graviton (which is of order $m^2 \sim \kappa\,\zeta$)[7]. On the other hand, this contribution from the interaction term can be compensated for by a finely-tuned contribution from the vacuum energy of matter fields, and then we can have an asymptotically flat solution with exactly the same form as for massless gravity.

It is therefore of some interest to understand the global structure of such solutions, whose analysis we defer to the next Section. The perturbative analysis and the investigation of stability of these solutions are left for future work [27]. Let us now turn our attention to diagonal solutions.

---

[7] See also the related discussion of Ref. [26]

2.2 Type II solutions

Type II solutions are defined as those which do not satisfy (11), and therefore must be diagonal. Although the general type II solution is not known, some progress can be made by further assuming that one of the metrics, say g, is a solution of

$$G^g_{\mu\nu} = \Lambda g_{\mu\nu}, \tag{24}$$

for some constant Λ. In the Appendix, we show that the only Type II solutions in this subclass are such that

$$f_{\mu\nu} = \gamma g_{\mu\nu}, \tag{25}$$

where γ is a constant (to be determined below).

Substituting (25) in (5-6) yields a diagonal energy-momentum tensor for both the g and the f metrics, with respective cosmological constants given by

$$\Lambda_g = -6\kappa_g \zeta \gamma^{4v}(-1+\gamma)(-1-2u+2\gamma u)/(2\gamma^2) + \kappa_g \rho_g, \tag{26}$$

$$\Lambda_f = -6\kappa_f \zeta \gamma^{-4u}(-1+\gamma)(1-2v+2\gamma v)/(2\gamma^2) + \kappa_f \rho_f. \tag{27}$$

Eq. (25) implies that the Einstein tensors for both metrics are identical, and thus

$$\Lambda_g = \gamma \Lambda_f. \tag{28}$$

This is an algebraic equation which determines γ in terms of the parameters in the Lagrangian.

For instance, in the case where the vacuum energies in both matter Lagrangians are set to zero $\rho_g = \rho_f = 0$, Eq. (28) becomes

$$(\gamma - 1)(-2u + (-1 - \kappa + 2u(1-\kappa))\gamma + 2\kappa u\gamma^2) = 0. \tag{29}$$

Here $\kappa = \kappa_g/\kappa_f$. In Ref. [22], the case with $u = 0$ was considered. In that particular case, the only solution of (29) is $\gamma = 1$, and therefore $\Lambda_f = \Lambda_g = 0$. This theory has solutions with $f = g$, where f is an arbitrary solution of the vacuum Einstein equations [22], and the maximally symmetric background can only be flat space. However, for $u \neq 0$, Eq. (29) has additional zeroes corresponding to the vanishing of the second factor, and therefore we have additional maximally symmetric bi-de Sitter or bi-AdS solutions (besides the flat space solution $\gamma = 1$), even in the case where the vacuum energies ρ_f and ρ_g vanish.

Solutions satisfying (24) and (25) exist for arbitrary interaction between both metrics [not necessarily of the form (2)]. The reason is that by assuming the ansatz where $f_{\mu\nu} = \gamma g_{\mu\nu}$, we necessarily have

$$T^g_{\mu\nu} = \frac{2}{\sqrt{g}} \frac{\delta S_{int}[f,g]}{\delta g^{\mu\nu}} = \Lambda_g(\gamma)\, g_{\mu\nu},$$

with constant Λ_g, and similarly for T^f. All that will change from one theory to the other is the form of the equation $\Lambda_g(\gamma) = \gamma \Lambda_f(\gamma)$ which determines γ. Maximally symmetric solutions of the form (25) in a class of bi-gravity theories have been previously considered in [7]. A similar argument can be made for multigravity theories, where one can always find solutions where all metrics are proportional to each other (see e.g. [28]).

6

As in the case of type I, both f and g solve Einstein's equations with a cosmological term. In this sense, there is no sign of a vDVZ discontinuity either, and one finds the usual Schwarzschild-(A)dS metrics, without modification. Unlike Type II solutions, here the two metrics share the same light cones and therefore their causal structure doesn't pose any novelties. The phenomenology and perturbative analysis of such solutions will be discussed in a separate publication [27]. [8]

3   Global structure of Type I solutions

In dealing with spacetimes with two different metrics, it is natural to worry about their compatibility from the causal point of view. For instance, there is a Type I solution where f is de Sitter, while g is Schwarzschild. The conformal diagrams of f and g look rather different, and the question is whether they can be combined at all. The purpose of this section is to investigate such combined causal diagrams, and the peculiarities which they may introduce. We shall see, for instance, that when the solution above is maximally extended, one can send a signal from a geodesically complete de Sitter space to another geodesically complete de Sitter space, by following geodesics of the companion Schwarzschild metric. Another peculiarity is that the maximal extensions we shall consider tend to raise issues of global hyperbolicity, even in cases where both metrics f and g are separately globally hyperbolic. Nevertheless, we find that there are no blatant violations of causality, in the sense that it is not possible to construct closed future directed time-like curves by combining geodesics of both metrics. In what follows, we shall illustrate the construction of the diagrams through three different examples.

The basic procedure is to maximally extend the geodesics of each metric, even when they reach the conformal boundary of the companion metric. The resulting causal structure will be illustrated by representing light-cones of one of the metrics in the conformal diagram of the other. The relevance of such light-cones is two-fold. First of all, matter which is coupled to one of the metrics must follow trajectories which are always inside of the future light cone from a given point. Second, in the limit of very short wavelength, the interaction term between both metrics becomes negligible compared with the graviton kinetic term. Hence, high frequency gravitons will follow null geodesics of the corresponding metric.

Before we proceed with the specific examples, we should briefly comment on a particular type of "singularity" which arises in certain bigravity solutions (again, even in cases where both metrics are separately smooth). Note that the metric (14) becomes complex in regions where $D^2 < 0$. As noted in [21], the coordinate singularity at $D = 0$ can be removed by a change of variables. This is of course true, since f is in the family of Schwarzschild-(A)dS metrics, which are everywhere smooth (except perhaps at $r = 0$ when $M_f \neq 0$). However, it does not seem to be possible to

---

[8]Assuming that (24) is valid, these are the only solutions of type II. This does not contradict the perturbative approach developed by Aragone and Chela-Flores [22], who considered spherically symmetric and diagonal solutions for f taking g as a fixed flat metric. The difference with the present case is that in their analysis g is not dynamical, and therefore there is no need for the tensor T_g to be proportional to the metric [as we have assumed, on account of (4) and (24)]. The analysis presented in the Appendix does not exclude the existence of diagonal spherically symmetric bigravity solutions, where f would have an asymptotic behaviour along the lines of [22]. It only shows that if such solutions exist, then the metric g will not be proportional to f; and neither one will be a solution of Einstein's equations with a cosmological constant.

find a change of variables which would remove the singularity from both metrics at once, in the vicinity of the point at which D^2 changes sign, and which would make both metrics real. The reason is that there are geodesics of g which invade the regions $D^2 < 0$ (with arbitrary slope, in fact). On such geodesics, the line element with respect to f is generically complex, and since the line element is a scalar, this fact cannot be changed by a coordinate transformation. To avoid a complex metric, we could try matching type I solutions with type II solutions at $D = 0$. This possibility is currently under investigation [27].

For most of this Section we shall assume $\beta = 1$, which ensures positivity of D for all choices of the potentials p and q, and therefore seems to be the most natural choice [21]. For certain potentials, however, there may be other special values of β for which the metric is everywhere real (as we shall see in Section 3.3).

3.1   de Sitter with Minkowski

Let us choose parameters in (17-18) so that $\Lambda_g = 0$ and $\Lambda_f > 0$. Then there is a Type I solution where g is Minkowski and f is de Sitter. The corresponding potentials in Eqs. (13-14) are given by

$$p = \frac{2\Lambda_f}{9} \, r^2 \equiv H^2 r^2, \qquad q = 0. \tag{30}$$

Note that each of the spacetimes, characterized respectively by the metrics (13) and (14) with the above defined potentials, has a maximal extension which is geodesically complete (trivial in the case of Minkowski). However, combining both together will be non-trivial because the static coordinates (t, r) (where we also include implicitly the angular part) cover the whole of Minkowski space, but not the whole of de Sitter. Hence, the conformal diagram for the extended de Sitter space accommodates all points for which the metric g is defined, but the converse is not true. To illustrate the causal structure, let us represent the light-cones of metric g in the conformal diagram of f. To this end, it is convenient to use Kruskal-type coordinates, (see e.g. [29])

$$U = -\left(\frac{1 - Hr}{1 + Hr}\right)^{1/2} e^{-H\tilde{t}}, \qquad V = \left(\frac{1 - Hr}{1 + Hr}\right)^{1/2} e^{H\tilde{t}}. \tag{31}$$

Note that this involves $\tilde{t}$ (and not t), the temporal coordinate in which f is diagonal. Eq. (31) maps the interior of the de Sitter horizon $Hr < 1$ into the quadrant $U < 0, V > 0$ of the plane (U, V). The future event horizon for an observer at $r = 0$ corresponds to $U = 0$, whereas the past event horizon corresponds to $V = 0$ (see Fig. 1). The quadrant $U > 0, V > 0$ which lies beyond the future event horizon, is similarly covered by the change of coordinates

$$U = \left(\frac{Hr - 1}{Hr + 1}\right)^{1/2} e^{-H\tilde{t}}, \qquad V = \left(\frac{Hr - 1}{Hr + 1}\right)^{1/2} e^{H\tilde{t}}. \tag{32}$$

The remaining quadrants can be obtained by changing the sign in the right hand side of Eqs. (31-32). As usual, we may perform the conformal re-scaling $T = \text{arctanh } V + \text{arctanh } U$, and $R = \text{arctanh } V - \text{arctanh } U$, so that the in the new coordinates the four quadrants lie in a square of finite size (see Fig. 1). The vertical boundaries correspond to $r = 0$, while the past and future

boundaries of the diagram correspond to $r = +\infty$ (which is a spacelike boundary). Note further that the coordinate system (t, r) only covers the $V > 0$ corner of the maximally extended de Sitter spacetime but also that it accomodates positive and negative values of U, so that it goes beyond the future event horizon. Thus, this coordinate system is similar, as far as the de Sitter metric is concerned, to the Eddington-Finkelstein coordinates of a black hole. At this point one might worry about a possible singularity due to the presence of the horizon. Indeed, as we discussed above, a coordinate singularity in one of the two metric cannot always be removed by a coordinate change that renders both metrics non singular. Here the situation is different, and in the coordinates (t, r), both metrics are smooth and regular everywhere where t and r take finite values. So the $U = 0$ part of the de Sitter horizon in the $V > 0$ corner does not result in a singularity in the bimetric theory. Things are however more involved for the $V = 0$ part of the horizon, as we will now see.

To this end, let us consider the light-cones in the Minkowski metric. Radial null geodesics are simply given by

$$t = \epsilon r + k \tag{33}$$

where $\epsilon = \pm 1$ corresponds to future and past directed null rays respectively. For $\epsilon = 0$ we obtain the space-like $t = k$ slices. In order to represent such geodesics in the conformal diagram for metric f, let us first express them in terms of $\tilde{t}$. For the potentials (30), Eq. (19) reads

$$\mathrm{d}\tilde{t} = \beta^{-1/2}\mathrm{d}t + \frac{Hr}{1 - H^2r^2}(\beta - 1 + H^2r^2)^{1/2}\,\beta^{-1/2}\mathrm{d}r. \tag{34}$$

For $\beta = 1$ this yields

$$\tilde{t} = t - r - \frac{1}{2H}\ln\left|\frac{1 - Hr}{1 + Hr}\right|. \tag{35}$$

The integration constant has been chosen so that $\tilde{t} = t$ at $r = 0$. For $\beta \neq 1$, Eq. (34) can also be integrated, but the expressions are a bit more cumbersome and we shall omit them in what follows. Note that the change of variables (35) is discontinuous at the de Sitter horizon. This is just as well, since the coordinates $\tilde{t}, r$ become singular at $r \equiv r_H = H^{-1}$, and we need to consider the Kruskal-type coordinates anyway. Substituting in (31) or in (32), we have

$$U = \left(\frac{Hr - 1}{Hr + 1}\right)e^{-H(t-r)}, \qquad V = e^{H(t-r)}. \tag{36}$$

As noted above, these expressions are valid both for $U \leq 0$ and $U \geq 0$ (with $V > 0$), and so they cover both quadrants (31) and (32) at once. Now, the radial geodesics are easily given in the U, V chart (as a curve parametrized by r) by substituting (33) into (36),

$$U = \left(\frac{Hr - 1}{Hr + 1}\right)e^{-Hk}e^{-H(\epsilon-1)r}, \qquad V = e^{Hk}e^{H(\epsilon-1)r}. \tag{37}$$

Future directed null rays of the Minkowski metric $t = r + k$, are simply straight lines at 45 degrees,

$$V = e^{Hk} = const.$$

On the other hand, past directed null geodesics $\epsilon = -1$, as well as the spacelike geodesics $\epsilon = 0$, have a rather non-trivial behavior which is illustrated in Fig. 1. For $Hr \ll 1$, the light-cone emanating from $r = t = 0$ (i.e. $k = 0$) has the same shape as in Minkowski space. However, at $Hr \sim 1$ the past directed light-cone opens up and turns around in the U, V plane. Beyond this turning point, "past directed" null rays of Minkowski start progressing towards the future in the de Sitter diagram! In particular, at large affine parameter, $Hr \to \infty$, both space-like and past directed null geodesics of Minkowski meet at the upper left corner of the conformal diagram, $U \to +\infty, V \to 0$, which belongs to the future boundary of de Sitter. In fact, the future timelike infinity i^+ of Minkowski is mapped into the upper right corner of the de Sitter diagram, the future null infinity $\mathcal{I}^+$ of Minkowski is mapped into the future null infinity of de Sitter (which is spacelike), the spacelike infinity i^0 and null past infinity $\mathcal{I}^-$ of Minkowski are both mapped to the upper left corner of the de Sitter diagram (see figure 2). The situation is more complicated for the past timelike infinity i^- of Minkowski. The latter is split into three pieces: a particle moving back in time along a $r = constant$ geodesic of Minkowski space-time would either go to the upper left corner of the de Sitter diagram if $r > r_H$, to the lower right corner if $r < r_H$, or to the $U = 0, V = 0$ central point if $r = r_H$. However, a given timelike trajectory in Minkowski, stemming from the infinite past ($t = -\infty, r = r_H$) can emanate in the de Sitter diagram from any point along the diagonal $V = 0$. The latter diagonal is then representing the whole of the past $r = r_H$ infinity of Minkowski. This can be better seen, plotting the null geodesics of de Sitter into a conformal diagram for Minkowski. Inverting (36),

$$ t = r + H^{-1} \ln V, \qquad r = \frac{UV + 1}{H(1 - UV)}, \tag{38} $$

outgoing (or incoming) null curves are given parametrically in terms of U (or V) by taking $V = k$ (or $U = k$). These are represented in Fig. 2. In particular, one sees that past directed $U = constant$ null lines can intersect the $V = 0$ curve anywhere, while they all asymptote the $r = r_H$ curve in the Minkowski diagram as t goes to $-\infty$.

We may then ask whether it is possible to construct a closed time-like curve by combining signals which propagate in the f metric with those propagating in the g metric. We defer this discussion to Section 3.4, where we show that this is not possible for general type I solutions.

A similar analysis can be performed for other values of β. For $\beta > 1$, D is everywhere real and the causal structure is quite similar to the one described above. A minor difference is that the light-cones of Minkowski geodesics are not at 45 degrees near the origin (as they were in Fig. 1). This can be easily seen from Eq. (19). On the other hand, for $\beta < 1$ the metric becomes complex in the region $H^2 r^2 < 1 - \beta$ (see Fig. 3).

Let us now consider the issue of global structure. As was stressed above, the coordinates (r, t) cover the full Minkowski space corresponding to the metric g, but only half of the conformal diagram for the extended de Sitter metric, corresponding to $V > 0$ (see Fig. 1a). This portion is by itself globally hyperbolic, since the $t = k$ surfaces are Cauchy surfaces for all geodesics of both metrics in this region. However, the region $V > 0$ is not geodesically complete, since the the null geodesics $U = const.$ of de Sitter reach $V = 0$ at finite affine parameter. To obtain a geodesically complete space-time, we can match the solution in the upper half of the conformal diagram with a solution in the lower half of the diagram. For this purpose we introduce a *second*
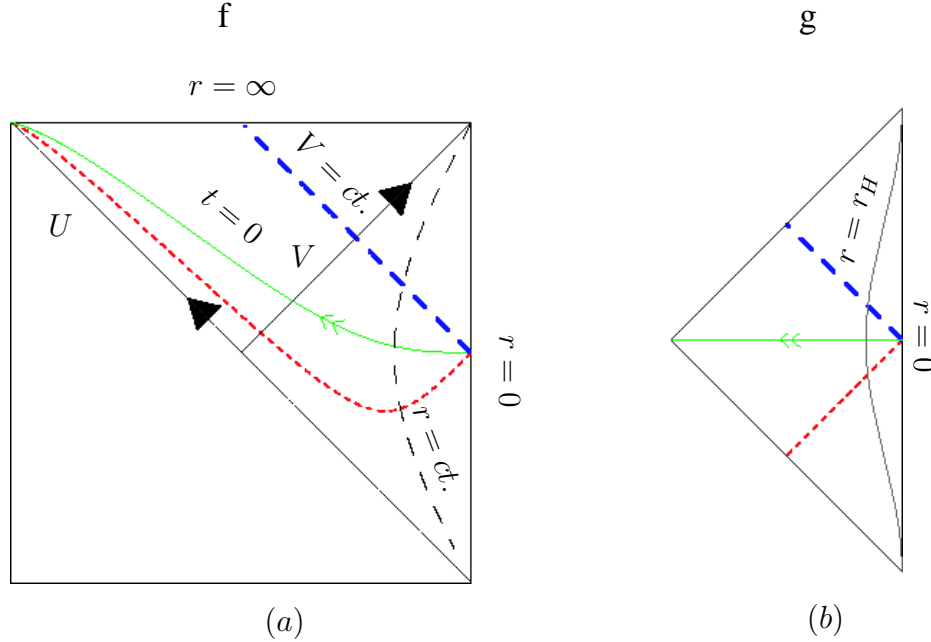
10

Figure 1: Causal diagrams when the f metric is de Sitter (left diagram) while the g metric is Minkowski (right diagram) and $\beta = 1$. The dashed curly vertical line of the left diagram represents a sphere of constant radial coordinate r. The solid curly vertical line of the right diagram represents the de Sitter horizon $r = r_H$ plotted in the Minkowski space-time. We also plotted three radial geodesics of Minkowksi space-time emanating from the origin $r = 0$ at $t = 0$: the thick dashed (blue) curve is a future-directed radial null ray from the origin (notice it is also a null geodesic ($V = $ constant) of the de Sitter space-time), the thin solid (green) curve with two arrows is a $t = 0$ radial geodesic, the thin dashed (red) curve is a past-directed null ray from the origin. The last two curves are radial geodesics of Minkowski space-time but not of de Sitter space-time. The whole of the Minkowski space-time is mapped onto the half of the de Sitter diagram verifying $V > 0$. Note that the past directed null geodesics of Minkowski turn around and start moving towards the future boundary of de Sitter space. This behaviour, however, does not lead to closed time-like curves, as discussed in Section 3.4

Minkowski space, with metric g', which will be covered with coordinates r' and t'. The change of variables (31) and (32) with the substitutions $t \to -t'$, $U \to -U$, $V \to -V$, maps the full range of the coordinates r', t' into the lower half of the de Sitter conformal diagram, below the diagonal $V = 0$. The full diagram, represented in Fig. 3, is now geodesically complete. In doing such an extension, we mean we are gluing together one Minkowski spacetime to the other along the past infinity of the $r = r_H$ sphere of the former to the future infinity of the $r = r_H$ sphere of the latter. These infinities do not belong to the Minkowski spacetimes, but to their boundaries, while they are located in the interior of the de Sitter spacetime. This provides indeed a perfectly fine geometric maximal extension, where all geodesics are complete.

We should add, however, that a maximal extension is usually required to satisfy the equations of motion. The bigravity equations of motion are certainly satisfied everywhere in regions I, II, III and IV of Fig. 3, but it is unclear in which sense they are satisfied along the diagonal $V = 0$. The problem is precisely that we are joining two Minkowski spacetimes [(a) and (c) of Fig. 3] at a locus
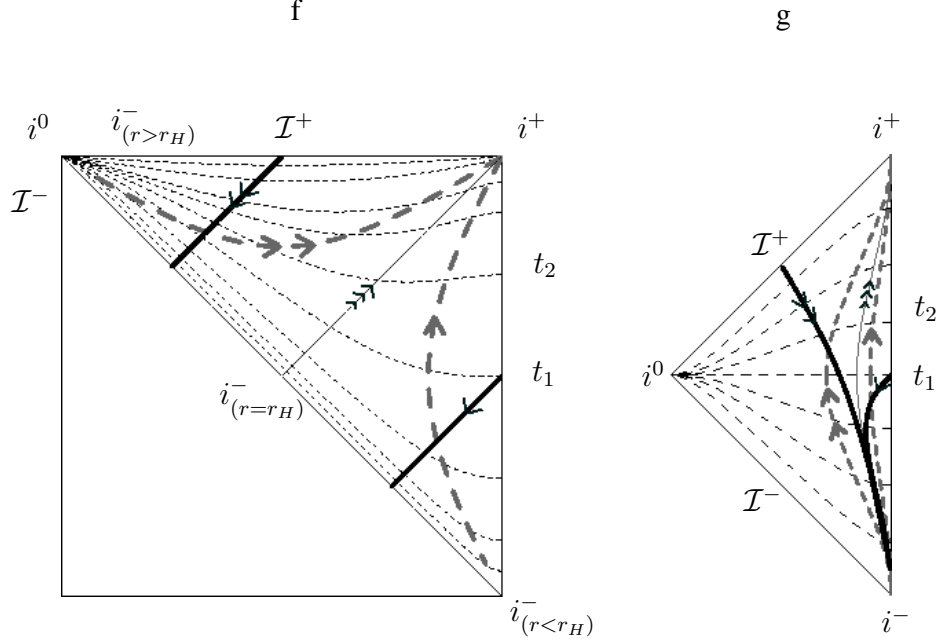
Figure 2: Causal diagram for de Sitter with Minkowski, for $\beta = 1$. The left diagram is for de Sitter with horizon radius r_H, while the right diagram is for Minkowski. The dashed thin lines (with no arrows) are $t = $ constant lines. The dashed thick line with one (resp. two) arrow is an $r = $ constant curve, with $r < r_H$ (resp. $r > r_H$). The thin solid line with three arrows represents the trajectory of an observer sitting at constant radius $r = r_H$ in Minkowski spacetime. The thick solid lines with arrows are past directed null geodesics of de Sitter space time $U = constant$ curves. The mapping of the infinities (null, spacelike, timelike) of Minkowski spacetimes ($i^{\pm,0}$, $\mathcal{I}^{\pm}$) has been indicated on the de Sitter diagram. One of the stricking feature of those diagrams, is that the past time-like infinity of Minkowski is split between the upper left corner (for $r > r_H$), the lower right corner (for $r < r_H$) and the diagonal ($r = r_H$) of the de Sitter space-time.

which lies at their conformal boundary. It is conceivable that promoting our maximal extension to a solution of the equations of motion might necessitate additional input, such as the inclusion of some source at the time-like infinity of Minkowski. Furthermore, as we shall see below, the extensions are not unique. This may seem surprising at first sight, but as we shall comment later on, a similar ambiguity is present in usual General Relativity when a metric must be continued beyond a Cauchy horizon.

Note that the extended diagram, Fig. 4, is not globally hyperbolic. The $t = k$ surfaces of the region $V > 0$ are no longer Cauchy surfaces for the whole space-time, since they do not intersect causal geodesics in the lower half of the diagram. A surface which intersects all causal geodesics should cut through both regions, $V > 0$ as well as $V < 0$. One such surface is, for instance, the horizontal line $U = V$. The problem is that, as can be seen in Fig. 4, there are geodesics which intersect this surface twice (such as the past directed null rays from $r = t = 0$). A formal proof that the maximally extended diagram of Fig. 4 is not globally hyperbolic runs as follows. Let us restrict attention to radial geodesics. A Cauchy surface must intersect all causal geodesics once and only once. Let us assume that such a surface Σ exists. In particular, Σ must intersect the
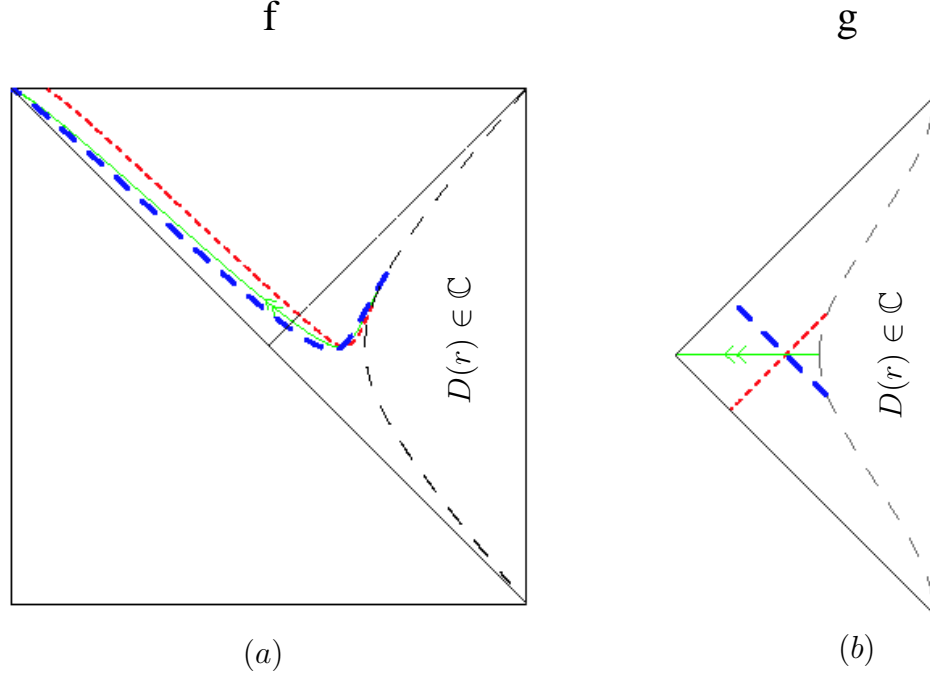
Figure 3: Causal diagrams when the f metric is de Sitter (left diagram) while the g metric is Minkowski (right diagram) and $\beta = 1/6$. Thick dashed (blue) curve, thin dashed (red) curve, and thin solid (green) curve with two arrows, are respectively null (for the two first) and spacelike (for the last) radial geodesics of Minkowski space-time. The dashed curly vertical line in both diagram is an $r = $ constant curve which is the boundary of the region where one of the metrics becomes complex.

null geodesic $V = 0$ of de Sitter space. By continuity, it will also intersect the null geodesics $V = const.$, in the range $-\delta < V < \delta$, where δ is an arbitrarily small positive number. Let us now consider the null geodesic of Minkowski space, parametrized by r in Eq. (37), and let us choose the constant $k < H^{-1} \ln \delta$. It is clear that the incoming radial geodesic (with $\epsilon = -1$) will start at the upper left corner of the de Sitter diagram (at $r \to \infty$), and work its way down towards the right boundary of the diagram (at r=0), while V will always remain in the interval $0 < V < \delta$). Hence, the incoming null geodesic must intersect Σ at least once before it reaches $r = 0$. At $r = 0$ it bounces and becomes the outgoing null geodesic $V = e^{Hk} < \delta$, which will intersect Σ once more before it reaches null future infinity. Hence, there are geodesics of Minkowski which intersect Σ twice, which simply means that this is not a good Cauchy surface for all geodesics in the extended diagram.

Let us compare the present situation to that in usual GR. As mentioned above, Cauchy horizons are also present in certain maximally extended solutions of GR, such as Reissner-Nordstrom or Anti de Sitter space. Whenever there is such a horizon, the equations of motion do not suffice to continue the solution past it, and we need additional input. Usually, analytic continuation is used, or else some boundary conditions at certain time-like boundaries of spacetime are introduced. As mentioned above, in the present context it is not clear whether the equations of motion are satisfied or not at the Cauchy horizon of the maximally extended solution, but this is precisely because
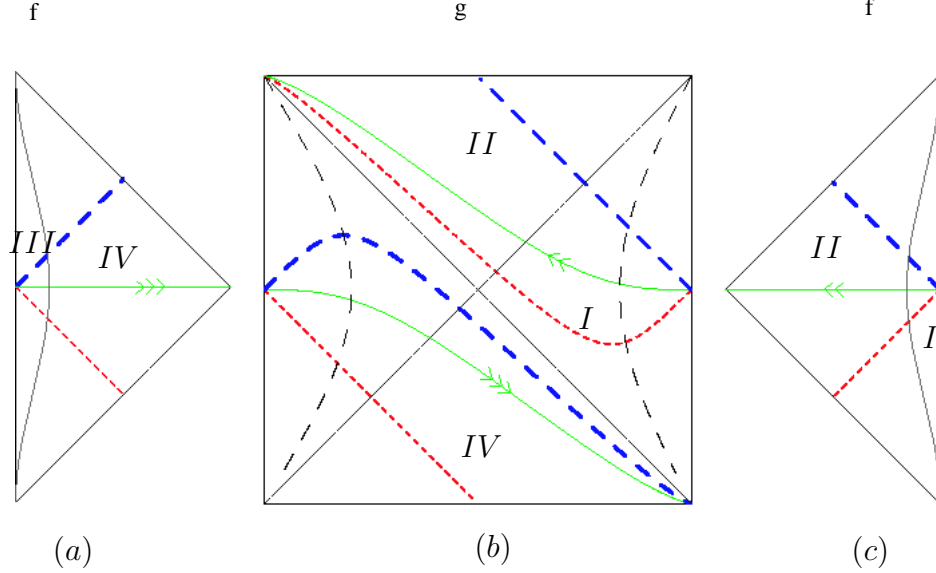
Figure 4: Diagram showing the extension proposed in the text for the de Sitter/Minkowski solution. Notations are the same as in Fig. 1. By using a second Minkowski space, we can extend the de Sitter diagram of Fig. 1, represented by region I and II above, to the lower half, represented by region III and IV above. The de Sitter space-time is now geodesically complete, however the whole space-time it is not globally hyperbolic, when both metric are considered on the same footing. If we draw a Cauchy surface for all the de Sitter geodesics [such as a horizontal line cutting accross the diagram (b)], this surface will intersect some of the Minkowski geodesics twice, while it will fail to intersect some others.

this horizon corresponds to a point in the conformal boundary of one of the metrics. In this sense, the situation is no worse than in GR, where we have to prescribe data on certain boundaries in order to determine the maximal extension. Another point to consider is that, physically, Cauchy horizons tend to be unstable to perturbations, because of large blueshift effects. The same is expected to happen in the present context. Note, e.g., from Fig. 4, that all future directed null geodesics of Minkowski in regions III and IV tend to pile up near the Cauchy horizon at $V = 0$, suggesting that there will be a large backreaction near that surface once we include perturbations [27].

Another interesting fact of the bi-metric solution is that the concepts of causal past and future are "broadened", since signals can be transmitted by matter coupled to both metrics. For instance, the observers at $r = 0$, with $V > 0$ can see signals emitted by all other observers, and hence they have no future event horizon. Likewise, observers at $r = 0$, with $V < 0$, can emit signals which will eventually reach all other observers, and hence they have no past event horizon. It is tempting to speculate that cosmological bi-gravity solutions, if they can be made sense of, could in principle be relevant to the horizon problem.

3.2 de Sitter with Schwarzschild

Let us now replace the Minkowski metric by the Schwarzschild one. In this case, the potentials of the Type I solution are given by

$$p = H^2 r^2, \qquad q = \frac{2M}{r}. \tag{39}$$

$$\tag{40}$$

Both metrics have now horizon singularities whenever $p = 1$ and $q = 1$, corresponding respectively to $r = r_H$ and $r = r_S \equiv 2M$. Those are coordinate singularities from the point of view of each metric considered separately from the other. However, one might be concerned by the possibility to remove such singularities from both metrics at the same time. To study this issue, we first keep p and q unspecified, and note that the coordinate change (19) reads (with $\beta = 1$, which we shall assume in the following) [9]

$$d\tilde{t} = dt - dr^* + d\tilde{r}^*, \tag{41}$$

r^* and $\tilde{r}^*$ defining "tortoise" coordinates associated with metric f and g respectively by

$$dr^* = \frac{dr}{1 - q} \tag{42}$$

$$d\tilde{r}^* = \frac{dr}{1 - p}. \tag{43}$$

Thus, introducing the null coordinates $v = t - r^*, u = t + r^*$ for the metric g, and $\tilde{v} = \tilde{t} - \tilde{r}^*, \tilde{u} = \tilde{t} + \tilde{r}^*$, for the metric f, one has from the above expression (41)

$$d\tilde{v} = dv. \tag{44}$$

This means that v is null for both metrics, but also that (v, r, θ, ϕ) are Eddington-Finkelstein coordinates for both metric. In such a coordinates system none of the metric is singular at the horizons.

Coming back to the explicit expressions for p and q (39) and substituting those in (19) we find

$$d\tilde{t} = \frac{1}{\sqrt{\beta}} \left\{ dt + \frac{\sqrt{(H^2 r^3 - 2M)(H^2 r^3 + (\beta - 1)r - 2\beta M)}}{(r - 2M)(1 - H^2 r^2)} dr \right\}, \tag{45}$$

For $\beta = 1$, we have

$$\tilde{t} = t - r^* - \frac{1}{2H} \ln \left| \frac{1 - Hr}{1 + Hr} \right|. \tag{46}$$

This matches equation (41) where, the Schwarzschild "tortoise" coordinate reads

$$r^* = r + 2M \ln |1 - r/2M|. \tag{47}$$

---

[9]we only discuss here the case $\epsilon_D = +1$, the other case, which corresponds to a change in the sign of time, follows similarly

The analog of Eq. (36) is now

$$U = \left(\frac{Hr - 1}{Hr + 1}\right)e^{-H(t-r^*)}, \qquad V = e^{H(t-r^*)}, \tag{48}$$

which, again, is valid both for $U > 0$ and $U < 0$ (with $V > 0$), covering both quadrants (31) and (32) of de Sitter, that is to say the region covered by the Eddington-Finkelstein coordinates (v, r, θ, ϕ). The null and spacelike radial geodesics of Schwarzschild can be written as

$$t = \epsilon r^* + k, \tag{49}$$

this being obviously valid in the whole region covered by coordinates (v, r, θ, ϕ). In the U, V chart these geodesics are given by

$$U = \left(\frac{Hr - 1}{Hr - 1}\right)e^{-Hk}e^{-H(\epsilon-1)r^*}, \qquad V = e^{Hk}e^{H(\epsilon-1)r^*}. \tag{50}$$

Again, we find that the null geodesics $t = r^*$ correspond to $V = const.$, (or $v = const$) so V is a null coordinate both in Schwarzschild and in de Sitter. The other radial geodesics, with $\epsilon = -1, 0$ have a more complicated form, which is qualitatively represented in Fig. 7. Note that for this figure, we have assumed that the Schwarzschild radius r_S is smaller that the de Sitter horizon radius r_H.

As we discussed previously, and is manifest from Fig. 6, half of the de Sitter diagram (above the diagonal) is mapped onto half of the Schwarzschild diagram (below the diagonal), corresponding to the region mapped by the Eddington-Finkelstein coordinates (v, r, θ, ϕ). Both half-diagrams are geodesically incomplete, since some geodesics reach the horizons (which dissects the diagrams in two) at finite affine parameter. These geodesics can of course be extended by adding new regions of spacetime. If one adds de Sitter and Schwarzschild regions, one obtains a "stair-case" diagram with an infinite chain of de Sitter and Schwarzschild space-times, two adjacent de Sitter (resp. Schwarzschild) space-times being linked together by a common Schwarzschild (resp. de Sitter) space-time. Needless to say, there is also a tension in this case between geodesic completeness and global hyperbolicity, as we found in the Minkowski-de Sitter case.

This seems to apply to more general situations where one of the metrics has an horizon which is not shared by the other one [27]. As noted previously, the new metric (new "step") which can be added to the stair does not necessarily correspond to the same solution as the one of the last step of the stair, since one of the two metrics does not determine uniquely the form of the other. Thus, in general we can construct "stair-case" diagrams with steps having different forms. Note further, that in the case considered here, the stairs can always be finished by adding a Minkowski spacetime, linked to a Schwarzschild space-time along a sphere of radius r_H at time-like infinity.

3.3 de Sitter with de Sitter

When both metrics are de Sitter, the potentials are given by

$$p = H_1^2 r^2 \qquad q = H_2^2 r^2. \tag{51}$$

16

For $\beta = 1$, the analysis proceeds along the same lines as in the previous Subsection, with the only difference that the (de Sitter) tortoise coordinate is now given by

$$r^* = -\frac{1}{2H_2} \ln \left| \frac{1 - H_2 r}{1 + H_2 r} \right|. \tag{52}$$

The corresponding causal diagram is represented in Fig. 9

Aside from the choice $\beta = 1$, the de Sitter de Sitter solution allows for another way of having $D^2 > 0$ for the entire range of r. Indeed, it is enough to have $H_1^2 \geq \beta H_2^2$ and $\beta \geq 1$ or $H_1^2 \leq \beta H_2^2$ and $\beta \leq 1$. Choosing for example β given by

$$\beta = \frac{H_1^2}{H_2^2}, \tag{53}$$

we have

$$H_1 \tilde{t} = H_2 t - \frac{1}{2} \ln \left| \frac{1 - H_1^2 r^2}{1 - H_2^2 r^2} \right|, \tag{54}$$

or $H_1(\tilde{t} - \tilde{r}^*) + \ln(1 + H_1 r) = H_2(t - r^*) + \ln(1 + H_2 r)$. Thus, the Kruskal coordinates (31-32) for the metric p can be expressed in terms of coordinates t and r as

$$U = \left(\frac{H_1 r - 1}{H_2 r + 1} \right) e^{-H_2(t - r^*)}, \qquad V = \left(\frac{H_2 r + 1}{H_1 r + 1} \right) e^{+H_2(t - r^*)}, \tag{55}$$

where r^* is given by (52). The corresponding diagram is given in Fig. 10.

3.4 Closed time-like curves?

An interesting question regarding the bigravity solutions is whether we can construct closed time-like curves by patching together geodesics corresponding to both metrics.

For $\beta = 1$ it is easy to show that this cannot be done, by using the "tortoise" coordinates r^* and $\tilde{r}^*$ that we defined in equations (42) and (43), as well as the null (for both metric) coordinate v (in all this subsection, we keep the functions p and q unspecified). The radial null and time-like geodesics of both metrics are given by

$$t = \epsilon r^* + k, \qquad \tilde{t} = \tilde{\epsilon} \tilde{r}^* + \tilde{k},$$

(Here $\epsilon = \pm 1, 0$ for outgoing and incoming null rays, or for spacelike geodesics, respectively, and similarly for $\tilde{\epsilon}$). Thus, any future directed causal curve with respect to f or g has the property that $dv \geq 0$, and dv vanishes only along the outgoing null radial geodesic. Once v increases, even if it is by just a little bit, it is impossible to go back to the original value by following a future directed time-like curve, which means that such curve cannot be closed.

Here, we disregard the possibility of making global identifications in the coordinate v, which might allow for the construction of a closed loop. Of course, even in flat space with a single metric, closed time-like curves could be constructed by global identifications, and in what follows we shall ignore this somewhat artificial setup. We shall only be concerned with the possibility of

17

locally constructing closed time-like curves within a given coordinate patch of space-time, without identifications.

To analyse the general case $\beta \neq 1$ it is convenient to separately consider the following regions of space-time:

a: For $(1 - p) < 0$, and $(1 - q) < 0$ the condition $\mathrm{d}r = 0$ defines a space-like surface for both metrics f and g. This means that r can only change monotonically along time-like curves of both metrics, making it impossible to close them in this region.

b: For $(1 - p) < 0$ and $(1 - q) > 0$, the condition $\mathrm{d}t = 0$ defines a space-like surface for the metric g. Also, from (19) with $\mathrm{d}t = 0$, we have

$$\left| \frac{d\tilde{t}}{d\tilde{r}^*} \right|^2 = 1 + \frac{1}{\beta} \left(\frac{1 - p}{1 - q} \right)^2 - \frac{\beta + 1}{\beta} \left(\frac{1 - p}{1 - q} \right) > 1. \tag{56}$$

Since $\tilde{t}$ is space-like in metric f this means that the surface $\mathrm{d}t = 0$ [which is also defined by Eq. (56)] is space-like in metric f too. Hence, t changes monotonically along time-like curves of both f and g, and as a consequence such curves cannot be closed.

c: If $(1 - p) > 0$ and $(1 - q) < 0$, then the surface $\mathrm{d}\tilde{t} = 0$ is space-like for f. From (19) with $\mathrm{d}\tilde{t} = 0$, we have

$$\left| \frac{\mathrm{d}t}{\mathrm{d}r^*} \right|^2 = 1 + \beta \left(\frac{1 - q}{1 - p} \right)^2 - (\beta + 1) \left(\frac{1 - q}{1 - p} \right) > 1. \tag{57}$$

Since t is space-like in metric g, Eq. (57) means that the surface $\mathrm{d}\tilde{t} = 0$ is space-like in metric g too, and $\tilde{t}$ must be monotonic on time-like curves, which therefore cannot close.

d: Finally, if $(1 - p) > 0$ and $(1 - q) > 0$, then we must distinguish two cases. For $p \geq q$, it is easy to see that $A > 0$ in Eq. (14), and therefore $\mathrm{d}t = 0$ is space-like for both metrics f and g. Hence, t is monotonic for time-like curves of both metrics. On the other hand, for $p \leq q$, Eq. (57) for $\mathrm{d}\tilde{t} = 0$ leads to

$$\left| \frac{\mathrm{d}t}{\mathrm{d}r^*} \right|^2 < 1. \tag{58}$$

Since now t is time-like in metric g, this means that $\mathrm{d}\tilde{t} = 0$ is a space-like surface for this metric. Of course $\mathrm{d}\tilde{t} = 0$ is also space-like for f, and so $\tilde{t}$ is monotonic along causal curves for both metrics.

This completes the proof for the individual regions listed above. It is remarkable that in spite of the strong differences in the light-cone structure of both metrics, it is not possible to draw closed time-like curves in any of the regions. The reason is that the future light-cone for one of the metrics never contains a part of the past light-cone for the other metric. Thus, we can always find a coordinate which labels hypersurfaces which are space-like for both metrics. This coordinate must grow monotonically along time-like curves.

By continuity, at the boundaries in between the regions, the future light-cone of one of the metrics can at most touch the past light-cone of the other metric, sharing perhaps a common null direction for both metrics. Even if this were the case, a future directed time-like geodesic with respect to one of the metrics can never get to the inside of the past light cone with respect to the other metric, and closed time-like curves cannot be constructed even if we cross the boundaries between the individual regions. [10]

---

[10] In the examples we have examined, the situation where the future light-cone of one of the metrics marginally

4 Conclusions

In this paper we have analyzed the global structure of a wide class of spherically symmetric bigravity solutions. We have reviewed their classification, pointing out that vacuum energy terms of the matter lagrangian can be included in type I solutions, and we have discussed a new subclass of type II solutions.

In order to probe the global structure of the solutions, the basic strategy has been to map the radial null geodesics of one of the metrics (say g) in the conformal diagram of the companion geometry (corresponding to metric f). The relevance of such geodesics is two-fold. First of all, they are followed by test particles of the matter sector coupled to each metric. Second, in the limit of high frequency, the interaction term between f and g is negligible compared with the kinetic term, and short wavelength gravitons will travel along the light cones of the corresponding metrics.

The results illustrate several intriguing features, originating in the different light-cone structure of metrics f and g. For instance, a *past directed* null geodesic of metric g may well end up at the *future* boundary of f, as happens in the case when f is de Sitter and g is Minkowski (Fig. 1). In spite of this seemingly bizarre behaviour, we have also shown that for all known solutions, it is not possible to construct closed time-like curves by piecing together geodesics of both metrics. The basic reason is that the future light cone with respect to one of the metrics never invades the interior of the past light cone with respect to the other metric.

Another peculiarity is that, even if metric f is geodesically complete by itself, some of its geodesics reach the conformal boundary of g at a finite value of their affine parameter. In order to extend them, further "copies" of the full conformal diagram of g can be incorporated. In some cases, this leads to an infinite chain of diagrams, such as the "stair-case" of Fig. 8, where adjacent de Sitter diagrams (corresponding to metric f) are linked together through a common Schwarzschild diagram (corresponding to metric g). In this maximally extended bigravity solution, one could send a message from one de Sitter space to the next by travelling along a geodesic of metric g.

The inclusion of several copies of the conformal diagram of a given metric leads, in general, to lack of global hyperbolicity, even when the "building block" diagrams are globally hyperbolic with respect to their own geodesics. Note, however, that global hyperbolicity breaks down in many exact solutions of ordinary General Relativity (GR), such as Reissner-Nordstrom or in Anti-de Sitter space. This is not necessarily a problem for practical applications, because usually only a part of the diagram will be relevant.

The concept of event horizon is broadened in the context of bi-metric solutions. In principle, through gravitational interactions, any observer will be affected at some level by signals propagating in either metric. In particular, a geodesic observer sitting at $r = 0$ in de Sitter space will have no future event horizon, provided that he or she is sensitive to the signals which are sent

---

touches the past light-cone of the other metric at the boundary between regions does not arise. If it did, then there might closed future-directed *null* curves at such boundary. Note, however, that since the boundary is at $r = const.$, this situation can only happen when both metrics have a common event horizon at the same value of r. The possibility of having closed null curves on these boundaries may require a case by case analysis, and is left for further research.

along the geodesics of Minkowski (see Fig. 1).

In summary, the global structure of bimetric solutions presents some unusual features which, nevertheless, do not seem more pathological than those encountered in maximally extended solutions of GR. It is interesting that all the bi-metric solutions considered are such that both metrics f and g are solutions of Einstein's equations with a cosmological term. Their possible phenomenological relevance seems therefore worthy of further consideration, and will be discussed elsewhere [27] (see also ref. [7]).

5 Acknowledgements

Appendix A: Type II solutions

Here we show that the most general Type II solution where one of the metrics satisfies (24), is such that $f_{\mu\nu} = \gamma g_{\mu\nu}$, where γ is a constant whose value is given by the equations of motion.

From (24), we have $KT_{tt}^g + JT_{rr}^g = 0$, and plugging expressions (7) and (8) into Eqs. (6), we have

$$KT_{tt}^g + JT_{rr}^g = \frac{\zeta B}{2r^4}\left(\frac{\Delta B^2}{JKr^4}\right)^{v-1}(AJ - CK)(3B - 2r^2) = 0. \qquad (59)$$

Since we are now assuming that $B \neq (2/3)r^2$, it follows that

$$AJ - CK = 0. \qquad (60)$$

Hence, from (7) and (8) plugged into (5),

$$AT_{tt}^f + CT_{rr}^f = -\frac{\zeta}{2B}\left(\frac{JKr^4}{\Delta B^2}\right)^u(AJ - CK)(3B - 2r^2) = 0, \qquad (61)$$

and from the equations of motion

$$AR_{tt}^f + CR_{rr}^f = 0. \qquad (62)$$

From this we obtain (see e.g. [21] for the explicit expressions of the Ricci tensor components),

$$-B'' + \frac{B'^2}{2B} + \frac{\Delta'B'}{2\Delta} = 0. \qquad (63)$$

A first integral is given by

$$\frac{B'^2}{B} = 4a^2\Delta \qquad (64)$$

20

where a is the constant of integration.

Let us now consider the linear combination

$$r^2 T_{tt}^g + J T_{\theta\theta}^g = -\frac{\zeta}{2Kr^2} \left(\frac{AB^2C}{JKr^4} \right)^{v-1} (BJ - Cr^2)(BK - 3AB + Ar^2), \tag{65}$$

which again must vanish if g is a is a solution of (24). Thus one either has

$$BK + Ar^2 = 3AB, \tag{66}$$

or

$$BJ = Cr^2. \tag{67}$$

In both cases

$$BT_{tt}^f + CT_{\theta\theta}^f = \frac{\zeta}{2AB} \left(\frac{JKr^4}{AB^2C} \right)^u (BJ - Cr^2)(BK - 3AB + Ar^2) = 0. \tag{68}$$

Note that (61) and (68) imply that $T_{\mu\nu}^f = H(r) f_{\mu\nu}$. The equations of motion require that T^f must be covariantly conserved, which implies that H is a constant. Therefore, f is a solution of Einstein's equations with a cosmological constant.

Consider first the case when (66) is satisfied. From this equation and (60), we can eliminate A and C as functions of B and $J = K^{-1}$. We get from (64)

$$\frac{B'^2}{B^3} = \frac{4a^2}{(3B - r^2)^2}. \tag{69}$$

With the change of variable

$$B(r) = r^2 F^2(r), \tag{70}$$

the differential equation (64) is written as

$$rF' = \frac{aF^2}{(3F^2 - 1)} - F, \tag{71}$$

which can be easily integrated to give

$$cr = \frac{1}{F} \left(\frac{\sqrt{12 + a^2} - a + 6F}{\sqrt{12 + a^2} + a - 6F} \right)^{\frac{a}{\sqrt{12+a^2}}}, \tag{72}$$

where c is an integration constant. Notice that

$$F(r) = (\sqrt{12 + a^2} + a)/6, \tag{73}$$

is a solution for $a > 0, c \to \infty$ and for $a < 0, c = 0$, which means

$$B \propto r^2. \tag{74}$$

21

In fact, as we shall see, Eq. (74) must hold in general. The equation of motion $BR_{tt}^f + CR_{\theta\theta}^f = 0$ takes the form [21]

$$BC'' - CB'' + 2\Delta + (CB' - BC')\frac{\Delta'}{2\Delta} = 0. \tag{75}$$

From (60) and (66), we have

$$A = \frac{BK}{3B - r^2}, \quad C = \frac{BJ}{3B - r^2}, \tag{76}$$

and hence

$$\Delta = \frac{B^2}{(3B - r^2)^2}. \tag{77}$$

Now, Eqs. (76) and (77) can be used in (75) in order to eliminate Δ and C in terms of B and its derivatives (as well as the known function J and its derivatives). The derivatives of B can be eliminated from (64), and with this Eq. (75) becomes an algebraic equation relating B and r. Substituting $B = r^2 F^2$, and then eliminating r from Eq. (72), we find an algebraic equation involving only F and the integration constants a and c. It turns out that this algebraic equation does *not* vanish identically. Indeed, the first terms in an expansion in powers of F are given by

$$BR_{tt}^f + CR_{\theta\theta}^f = \frac{J(r)F(r)}{(3F(r)^2 - 1)^4 r}\left(\left(\frac{\sqrt{12 + a^2} - a}{\sqrt{12 + a^2} + a}\right)^{\frac{3a}{\sqrt{12+a^2}}} c^{-3}\Lambda_g \right.$$
$$\left. + \left\{2a\left(\frac{\sqrt{12 + a^2} - a}{\sqrt{12 + a^2} + a}\right)^{\frac{a}{\sqrt{12+a^2}}} c^{-1} + 9a\left(\frac{\sqrt{12 + a^2} - a}{\sqrt{12 + a^2} + a}\right)^{\frac{3a}{\sqrt{12+a^2}}} c^{-3}\Lambda_g - 6M\right\}F + O(F^2)\right),$$

where we have used $J = 1 - 2M/r + \Lambda_g r^2/3$. For the zeroth and first order to cancel identically, one needs

$$\Lambda_g = 0, \quad M = \frac{ac^{-1}}{3}\left(\frac{\sqrt{12 + a^2} - a}{\sqrt{12 + a^2} + a}\right)^{\frac{a}{\sqrt{12+a^2}}}, \tag{78}$$

but then going to the next order in F the expression (75) does not cancel for any value of a. Thus, F is fixed to be a constant whose value is determined by (75). From this (74) follows.[11] Now, it is easy to show that whenever $B \propto r^2$ both metrics must be proportional to each other. Indeed, it follows from Eq. (64) that $\Delta = AC = const.$ and $B = (a^2\Delta)r^2$. Also, using $JK = 1$ and (60) we have $A = \Delta^{1/2}K$ and $C = \Delta^{1/2}J$. On the other hand, for constant Δ, Eq. (75) reads

$$BC'' - CB'' + 2\Delta = 0.$$

Using $B = (a^2\Delta)r^2$, $C = \Delta^{1/2}J$ and $J = 1 - 2M/r + \Lambda_g r^2/3$, where M and Λ_g are constants, it follows immediately that $a^2 = \Delta^{-1/2}$, which implies $B = \Delta^{1/2}r^2$. It is then clear that $f_{\mu\nu} = \gamma g_{\mu\nu}$, where $\gamma = \Delta^{1/2}$ is a constant, as we intended to show.

---

[11]Provided, of course, that the algebraic equation has any solution at all. Otherwise there simply aren't any solutions under the assumption (66). Note, in particular, from (72) and the subsequent discussion, that the constancy of F can only be achieved for very special values of the integration constants, but these turn out to be the only relevant ones.

Next, let us consider the case (67). Here, we can use (60) and (64) to obtain

$$\frac{B'^2}{B^3} \propto \frac{1}{r^4},$$

(79)

and equation (79) yields

$$B = \frac{\gamma r^2}{(1 + \alpha r)^2}.$$

(80)

Since we have assumed that g satisfies Einstein's equations with a cosmological constant, Eq. (24), $T^g_{\mu\nu}$ should be proportional to $g_{\mu\nu}$ with a constant proportionality factor. This is achieved only for $\alpha = 0$ which means $C = \gamma J$. This means that both metrics will be proportional, with

$$f_{\mu\nu} = \gamma g_{\mu\nu}.$$

(81)

This completes our proof.

As discussed in the text, the remaining equations of motion determine the constant γ in terms of the parameters in the Lagrangian.

References

[1] G. R. Dvali, G. Gabadadze and M. Porrati, Phys. Lett. B **485** (2000) 208 [arXiv:hep-th/0005016].

[2] T. Damour and I. I. Kogan, Phys. Rev. D **66** (2002) 104024 [arXiv:hep-th/0206042].

[3] N. Arkani-Hamed, H. C. Cheng, M. A. Luty and S. Mukohyama, JHEP **0405**, 074 (2004) [arXiv:hep-th/0312099].

[4] V. A. Rubakov, arXiv:hep-th/0407104.

[5] S. L. Dubovsky, JHEP **0410**, 076 (2004) [arXiv:hep-th/0409124].

[6] C. Deffayet, Phys. Lett. B **502** (2001) 199 [arXiv:hep-th/0010186]. C. Deffayet, G. R. Dvali and G. Gabadadze, Phys. Rev. D **65** (2002) 044023 [arXiv:astro-ph/0105068].

[7] T. Damour, I. I. Kogan and A. Papazoglou, Phys. Rev. D **66**, 104025 (2002) [arXiv:hep-th/0206044].

[8] S. L. Dubovsky, P. G. Tinyakov and I. I. Tkachev, Phys. Rev. D **72** (2005) 084011 [arXiv:hep-th/0504067].

[9] M. Fierz, Helv. Phys. Acta 22 (1939) 3; M. Fierz and W. Pauli, Proc. Roy. Soc. Lond. A **173**, 211 (1939).

[10] C. J. Isham, A. Salam and J. Strathdee, Phys. Rev. D **3** (1971) 867.

[11] N. Arkani-Hamed, A. G. Cohen and H. Georgi, Phys. Rev. Lett. **86** (2001) 4757 [arXiv:hep-th/0104005]. C. T. Hill, S. Pokorski and J. Wang, Phys. Rev. D **64** (2001) 105005 [arXiv:hep-th/0104035].

[12] N. Arkani-Hamed, H. Georgi and M. D. Schwartz, Annals Phys. **305** (2003) 96 [arXiv:hep-th/0210184]. N. Arkani-Hamed and M. D. Schwartz, Phys. Rev. D **69**, 104001 (2004) [arXiv:hep-th/0302110]. M. D. Schwartz, Phys. Rev. D **68**, 024029 (2003) [arXiv:hep-th/0303114]. C. Deffayet and J. Mourad, Phys. Lett. B **589** (2004) 48 [arXiv:hep-th/0311124].

[13] H. van Dam and M. J. Veltman, Nucl. Phys. B **22** (1970) 397. V.I.Zakharov, JETP Lett **12**, 312 (1970). Y. Iwasaki, Phys. Rev. D **2** (1970) 2255.

[14] A. I. Vainshtein, Phys. Lett. B **39** (1972) 393.

[15] G. R. Dvali, G. Gabadadze and M. Porrati, Phys. Lett. B **485**, 208 (2000) C. Deffayet, G. R. Dvali, G. Gabadadze and A. I. Vainshtein, Phys. Rev. D **65** (2002) 044026 [arXiv:hep-th/0106001]. A. Lue, Phys. Rev. D **66** (2002) 043509 [arXiv:hep-th/0111168]. A. Gruzinov, New Astron. **10** (2005) 311 [arXiv:astro-ph/0112246]. M. Porrati, Phys. Lett. B **534** (2002) 209 [arXiv:hep-th/0203014]. T. Tanaka, Phys. Rev. D **69** (2004) 024001 [arXiv:gr-qc/0305031]. G. Gabadadze and A. Iglesias, Phys. Rev. D **72** (2005) 084024 [arXiv:hep-th/0407049].

[16] T. Damour, I. I. Kogan and A. Papazoglou, Phys. Rev. D **67**, 064009 (2003) [arXiv:hep-th/0212155].

[17] D. G. Boulware and S. Deser, Phys. Rev. D **6** (1972) 3368.

[18] C. Deffayet and J. W. Rombouts, Phys. Rev. D **72** (2005) 044003 [arXiv:gr-qc/0505134].

[19] P. Creminelli, A. Nicolis, M. Papucci and E. Trincherini, JHEP **0509** (2005) 003 [arXiv:hep-th/0505147].

[20] A. Salam and J. Strathdee, Phys. Rev. D **16**, 2668 (1977).

[21] C. J. Isham and D. Storey, Phys. Rev. D **18**, 1047 (1978).

[22] C. Aragone and J. Chela-Flores, Nuovo Cimento **10A** 818 (1972); J. Chela-Flores, Int. J. Theor. Phys. **10**, 103 (1974)

[23] J. J. van der Bij, H. van Dam and Y. J. Ng,**116A**, 307 (1982).

[24] A. Zee, in *High Energy Physics: Proceedings of the 20th Annual Orbis Scientiae*, 1983 edited by S.L. Mintz and A. Perlmutter (Plenum, New York). W. Buchmuller and N. Dragon, Phys. Lett. B **207**, 292 (1988). W. Buchmuller and N. Dragon, Phys. Lett. B **223**, 313 (1989).

[25] S. Weinberg, Rev. Mod. Phys. **61**, 1 (1989).

[26] G. Gabadadze and A. Gruzinov, Phys. Rev. D **72** (2005) 124007 [arXiv:hep-th/0312074].

[27] D. Blas, C .Deffayet, J. Garriga, *in preparation.*

[28] C. Deffayet and J. Mourad, Class. Quant. Grav. **21**, 1833 (2004) [arXiv:hep-th/0311125].

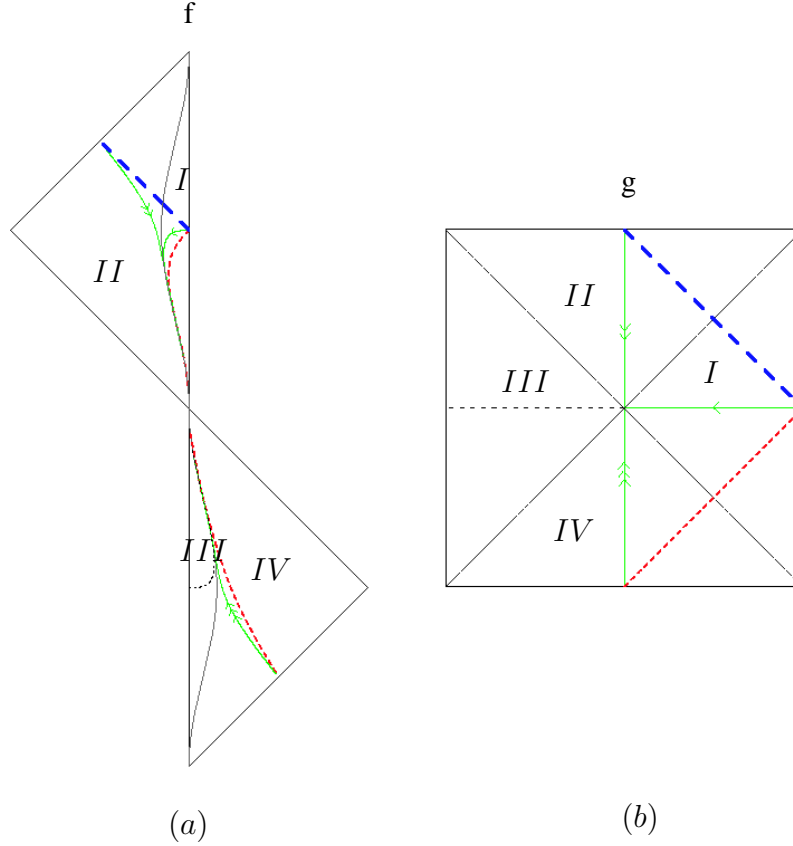[29] G. W. Gibbons and S. W. Hawking, Phys. Rev. D **15** (1977) 2738.

Figure 5: Same as Fig. 4, with radial geodesics of de Sitter plotted instead of those of Minkowski. The thick dashed (blue) curve is a future-directed radial null ray from the origin ($r = 0, \tilde{t} = 0$). The thin solid (green) curve is a $\tilde{t} = 0$ radial geodesic of de Sitter. The thin dashed (red) with one arrow curve a the past-directed null geodesic from the origin. We also plotted, as thin solid (green) curves with two and three arrows, the continuation of the $\tilde{t} = 0$ curve beyond the horizon $r = r_H$. When mapped into the Minkowski diagram, the past directed null geodesics of de Sitter, of region I, reach the timelike past infinity of the Minkowski space-time at a finite value of their affine parameter in de Sitter, namely when they cross the de Sitter horizon $r = r_H$. Nevertheless, we can "smoothly" continue them in the newly added Minkowski solution onto which regions III and IV of de Sitter space-time are mapped.
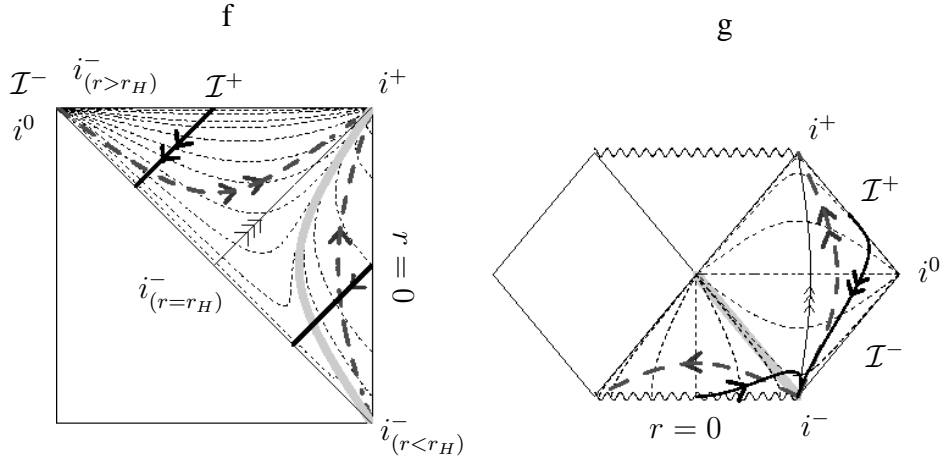
Figure 6: Causal diagrams when the f metric is de Sitter (right) and the g metric is Schwarzschild (left). The notations are the same as in figure 2. The main difference with the case depicted in this last figure is the presence of the Schwarzschild horizon. The part of the Schwarzschild horizon shown as a thick gray line on the right diagram above is mapped to the thick gray line of the left diagram. The part of the Schwarzschild horizon which is the diagonal of the right diagram orthogonal to the thick gray line is mapped to the upper right corner of the de Sitter diagram in analogy to what was found to happen for the de Sitter horizon when the other metric is Minkowski. This shows the possibility to extend the Schwarzschild space-time through another de Sitter spacetime joined to the other by the future infinity of a $r = r_S$ sphere (r_S being the Scharzschild horizon)
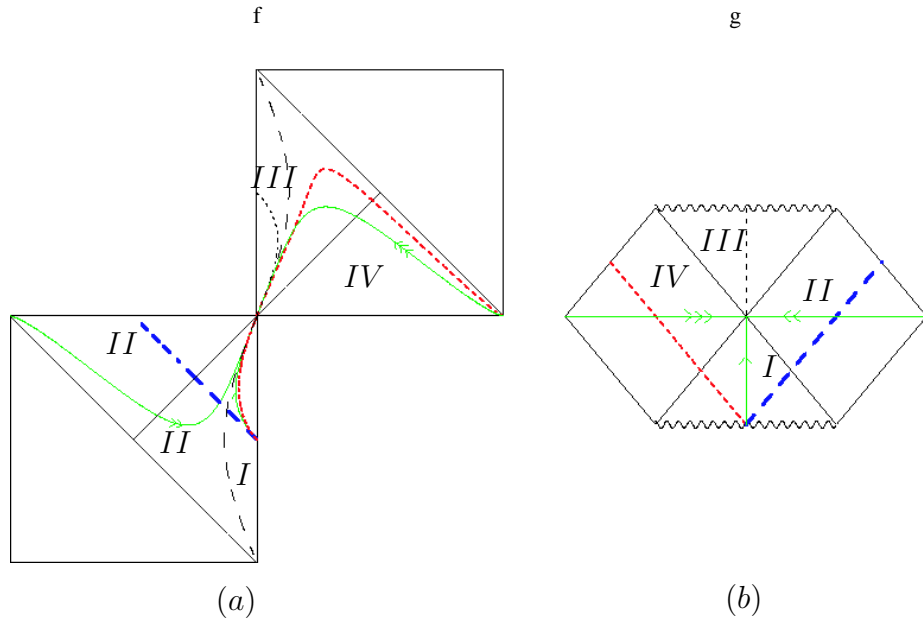
Figure 7: Causal diagrams when the f metric is de Sitter (right) and the g metric is Schwarzschild (left) showing the extension proposed in the text for the Schwarzschild space-time. Various radial geodesics of Schwarzschild are mapped onto the de Sitter diagram The dashed vertical curly line in the de Sitter diagrams indicates the Schwarzschild horizon. Note that we can "send a signal" from region I of the lower de Sitter space to region IV of the upper de Sitter space by using the left-moving null geodesic of Schwarzschild (thin dashed (red) line).
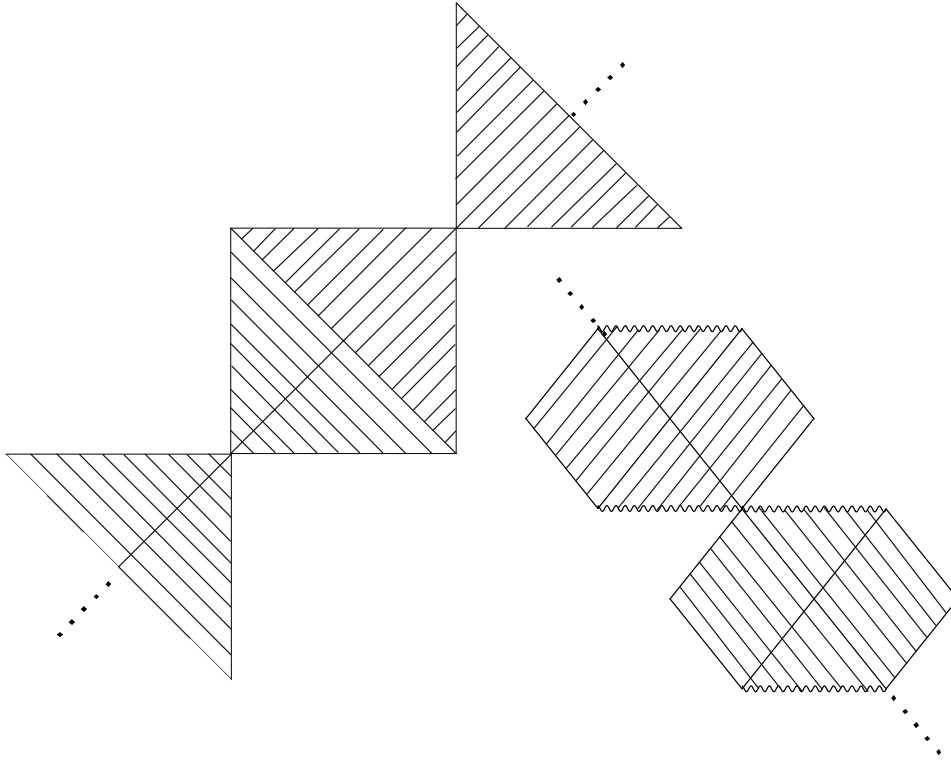
Figure 8: This shows a possible maximal extension of the bi-metric space-times, following the procedure given in the text, when one of the metric is de Sitter while the other is Schwarzschild. We are led to the "stair-case" diagram, an infinite chain of de Sitter spaces linked to each other through a common Schwarzschild diagram.
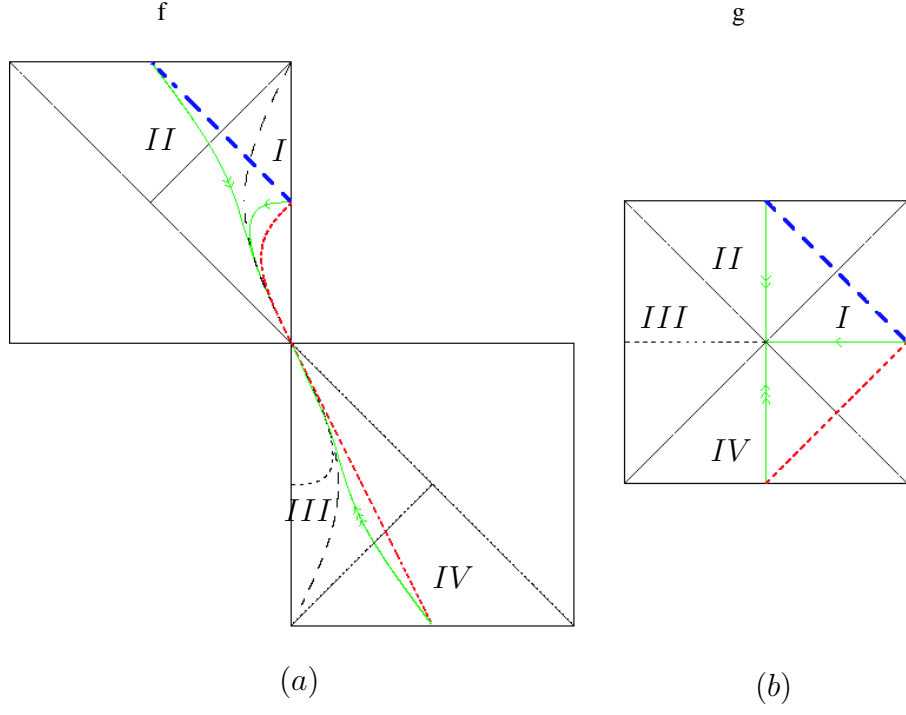
f   g

(a)   (b)

Figure 9: Causal diagram when both metric are de Sitter and $\beta = 1$. Notations are the same as in figure 5.

f   g
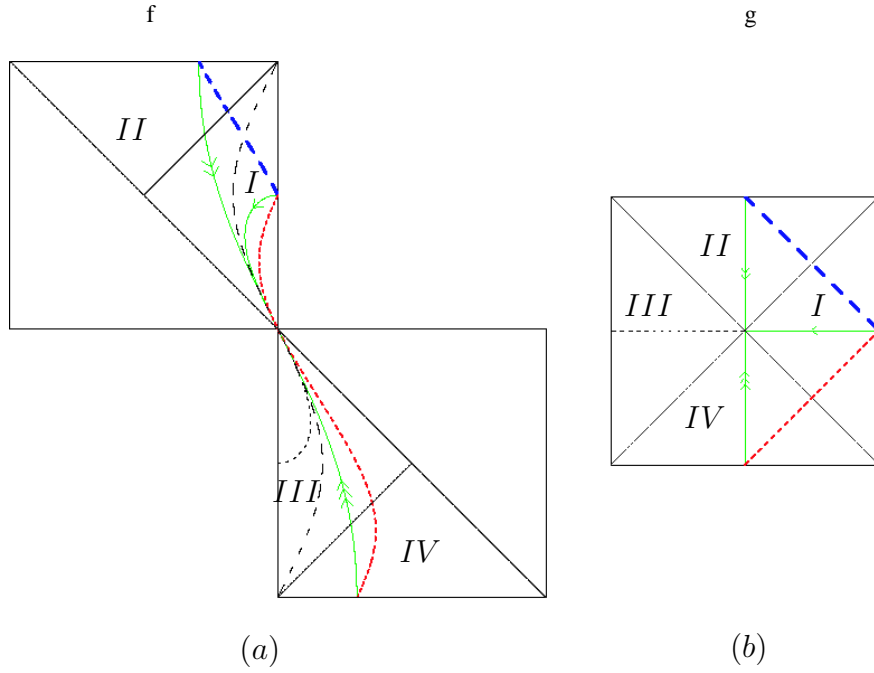
(a)   (b)

Figure 10: Causal diagram when both metric are de Sitter and $\beta = 1/4$. Notations are the same as in figure 5.